

C80-105

Strainrange Partitioning Behavior of an Advanced Gas Turbine Disk Alloy AF2-1DA

G.R. Halford* and A.J. Nachtigall*

NASA Lewis Research Center, Cleveland, Ohio

The low-cycle, creep-fatigue characteristics of the advanced gas turbine disk alloy AF2-1DA have been determined at 1400°F and are presented in terms of the method of Strainrange Partitioning (SRP). The mean stresses which develop in the PC- and CP-type SRP cycles at the lowest inelastic strain range were observed to influence the cyclic lives to a greater extent than the creep effects and hence interfered with a conventional interpretation of the results by SRP. A procedure is proposed for dealing with the mean stress effects on life which is compatible with SRP.

Nomenclature

A	= ratio of amplitude to mean
b	= fatigue strength exponent
BCCR	= balanced cyclic creep-rupture test (CC-type cycle)
CC	= tensile creep reversed by compressive creep
CCCR	= compressive cyclic creep-rupture test (PC-type cycle)
CP	= tensile creep reversed by compressive plasticity
D_C	= creep-rupture ductility
D_p	= tensile plastic ductility
HRLC	= high rate load cycling test (PP-type cycle)
HRSC	= high rate strain cycling test (PP-type cycle)
k	= transition function
N_{CC}	= cycles to failure for CC-type cycle
N_{CP}	= cycles to failure for CP-type cycle
N_f	= cycles to failure
N_{fm}	= cycles to failure in presence of mean stress
N_{f0}	= cycles to failure under zero mean stress
N_{PC}	= cycles to failure for PC-type cycle
N_{PP}	= cycles to failure for PP-type cycle
PC	= tensile plasticity reversed by compressive creep
PP	= tensile plasticity reversed by compressive plasticity
R	= ratio of algebraic minimum to maximum
TCCR	= tensile cyclic creep-rupture test (CP-type cycle)
V	= ratio of mean to amplitude
V_{eff}	= effective value of V_σ in presence of inelastic strains
V_ϵ	= ratio of mean strain to strain amplitude
V_σ	= ratio of mean stress to stress amplitude
ϵ	= axial strain
$\Delta\epsilon_{CC}$	= inelastic strain range of the CC-type
$\Delta\epsilon_{CP}$	= inelastic strain range of the CP-type
$\Delta\epsilon_{el}$	= elastic strain range
$\Delta\epsilon_{in}$	= inelastic strain range
$\Delta\epsilon_{PC}$	= inelastic strain range of the PC-type
$\Delta\epsilon_{PP}$	= inelastic strain range of the PP-type
σ	= axial stress
σ_a	= alternating stress amplitude
σ_f'	= fatigue strength coefficient
σ_m	= mean stress

σ_{max}	= maximum stress
σ_{min}	= minimum stress
σ_{ult}	= ultimate tensile strength
σ_y	= 0.2% offset yield strength
$\Delta\sigma$	= stress range = $2\sigma_a$

Introduction

AN increased interest has recently developed in the creep-fatigue crack initiation resistance of alloys for gas turbine disks. The interest is sparked by the steadily escalating use temperatures of disks, particularly near the rim in the blade root attachment area for high-performance military aircraft engines. Since disk alloys begin to experience creep deformation under high stresses at temperatures as low as 1100-1200°F, it is desirable that the creep-fatigue characteristics of such alloys be determined and made available for use in alloy selection and disk design. Early results of an evaluation of the high-temperature, creep-fatigue behavior of an advanced gas turbine disk alloy AF2-1DA are presented herein. A high temperature of 1400°F was selected to accelerate the creep process and permit an experimental testing program to be conducted in a reasonably short period of time. It should be emphasized that this study is directed toward achieving an increased understanding of material behavior as opposed to the generation of directly applicable design data. As such, it was convenient to exaggerate testing conditions beyond those expected in service in order to accelerate the effects of the variables under investigation. To date, the creep-fatigue behavior in the high-strain, low-cycle regime has only been determined. Here, the magnitude and type of the cyclic inelastic strain ranges are measured or controlled during testing and usually can be regarded as the dominant life-controlling variables. The method of Strainrange Partitioning (SRP)¹⁻³ was used as the vehicle for interpreting the creep-fatigue characteristics.

Since substantial mean stresses were involved in some of the creep-fatigue cycles employed in this investigation, a considerable amount of attention was given to assess their likely influence on cyclic life. Of particular concern is the simultaneous effect on cycle life of two important factors—mean stress and creep-fatigue interaction. Individually, these factors are known to have pronounced effects on cyclic life, but their combined influence is not well known. In this paper, these effects are addressed and a rationale for dealing with mean stresses in the presence of creep-fatigue interaction is proposed.

Experimental Details

The material acquired for this evaluation is the powder metallurgy product, GATORIZED AF2-1DA, an advanced

Presented as Paper 79-1192 at the AIAA/SAE/ASME 15th Joint Propulsion Conference, Las Vegas, Nev., June 18-20, 1979; submitted July 19, 1979; revision received Jan. 8, 1980. This paper is declared a work of the U.S. Government and therefore is in the public domain.

Index categories: Materials, Properties of; Structural Durability (including Fatigue and Fracture); Structural Design.

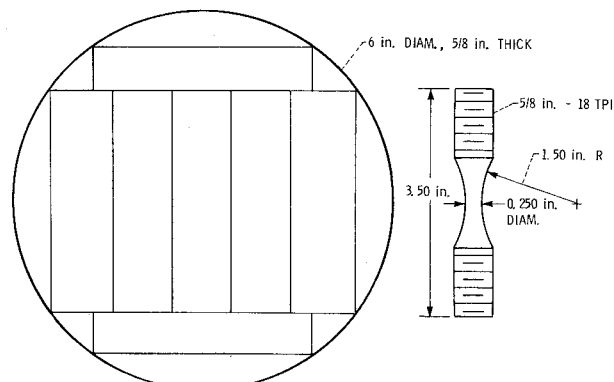
*Materials Engineer, Fatigue Research Section.

Table 1 Mechanical properties of AF2-1DA at 1400°F

Tensile properties		
Elastic modulus		$= 25 \times 10^3$ ksi
Yield strength (0.2% offset)		$= 123.4$ ksi
Ultimate tensile strength		$= 163.7$ ksi
Reduction of area		$= 22.3\%$
Stress-rupture properties		
Stress, ksi	Reduction of area, %	Time to rupture, h
135.0	15.8	1.1
130.0	14.6	2.1
125.0	15.0	196.1

nickel-base superalloy developed for use in gas turbine disks. The material was supplied to NASA in the fully heat-treated condition by Pratt & Whitney Aircraft Group, Government Products Division, under Contract NAS3-20947, 1978. A total of 36 pancakes were supplied (6 in. diameter \times 5/8 in. thick). The alloy was prepared from powder conforming to AMS-5855 both in density and particle size. The powder was canned and soaked for 8 h at 2000°F prior to extrusion. Extrusions were cut to size and creep-formed by the Gatorizing process at 2050°F into pancakes at a strain rate of 5%/min. The heat treatment was as follows: Heat from ambient to 2075°F in a vacuum and hold for 45 min. Then heat from 2075 to 2200°F at a rate of 1 deg/min, and hold at 2200°F for 1 h, followed by an argon quench. The AMS-5856 stabilization and precipitation heat-treat cycle consisted of the following: 2050°F/2 h/AC + 1300°F/12 h/AC + 1500°F/8 h/AC. The pancakes were used to make hourglass-shaped test specimens. Seven specimens were cut from each pancake in accordance with the layout and dimensions shown in Fig. 1. These specimens were used for tensile, creep-rupture, and fatigue tests. Tensile and creep-rupture results are summarized in Table 1.

Conventional creep-rupture tests were conducted using furnace heating, whereas the tensile and fatigue tests were conducted in closed-loop, servocontrolled, electrohydraulic testing machines using direct-resistance heating of the specimen. In these latter tests, the reported test temperature was monitored using an optical pyrometer aimed at the hottest point on the specimen (at the minimum diameter). Feedback control for the temperature was accomplished with the aid of a thermocouple spot-welded directly to the specimen surface at a point removed from the minimum diameter. A diametral extensometer was used to measure the strains in the tensile and fatigue tests. Further details of the testing facility and procedures have been described by Hirschberg.⁴

**Fig. 1 Specimen layout and dimensions.**

The basic low-cycle, creep-fatigue tests were performed in strict accordance with the guidelines set forth by Hirschberg and Halford³ for the evaluation of the SRP characteristics of an alloy. These tests were conducted using completely reversed strain cycles. Schematic stress-strain hysteresis loops are shown in Fig. 2 for the types of cycles used in conducting the tests to establish the SRP life relationships.

The strain-controlled PP-type test cycles were applied using a sinusoidal strain vs time waveform at a frequency of 0.5 Hz. In analyzing the results of the PP-type tests, it was assumed that the imposed strain rates were high enough to preclude the occurrence of creep strain, thus producing inelastic strains that could be classified as plasticity. For the PC-, CP-, and CC-type cycles, the creep strain was imposed by controlling the load on the specimen at a constant value until the desired creep strain limit was reached, whereupon, the loading direction was reversed and the other half of the cycle was imposed. If it was desired to impose creep strain in this portion of the cycle, the load was again held at a constant value until the desired opposite creep strain limit was attained, or if plasticity was desired, the specimen was rapidly loaded until the opposite strain limit was reached.

Additional tests were conducted to investigate the effects of mean stresses. Some tests were strain controlled, while others were load controlled. All were conducted at a frequency of 0.5 Hz using a sine wave.

Basic SRP Results

The high-temperature, low-cycle, creep-fatigue results from the basic SRP-type tests are documented fully in Table 2(a). In this paper, the results are interpreted only in terms of the SRP approach to high-temperature, creep-fatigue crack initiation, although alternate approaches, such as the time- and cycle-fraction rule,⁵ frequency modification,⁶ damage rate,⁷ etc., could be applied if so desired, based upon the information documented in the tables. The inelastic strain range is plotted against cyclic life in Fig. 3 for all four types of tests. This is simply a display of the raw data.

It is seen that there is a relatively small influence of the type of test on the cyclic life at inelastic strain range above 0.001, whereas below this level, the PC-type tests exhibit significantly lower lives than the other types. Furthermore, the CP-type tests appear to have lives that are not appreciably different from those of the PP-type tests, although, the data generated to date are sparse. These two observations are similar to previous findings for the nickel-base superalloys reported by a number of investigators in a recent NATO/AGARD Symposium on Strainrange Partitioning,⁸ but are opposite to the behavior noted for lower strength, higher ductility alloys, notably the austenitic stainless steels.⁹ Suggestions as to why the PC cycling is more severe than the CP were discussed briefly at the NATO/AGARD Symposium.

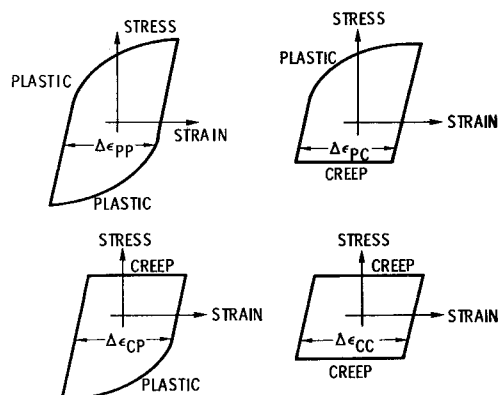
**Fig. 2 Idealized hysteresis loops for the four basic types of SRP cycles.**

Table 2 High-temperature, low-cycle creep-fatigue data for Gatorized AF2-1DA, 1400°F

TEST	AVG. FREQ., HZ.	AVG. HOLD TIME, SEC.		STRESS VALUES, σ				STRAINRANGE VALUES, $\Delta\epsilon$, %								N_F , CYCLES	t_F , HRS.
		TEN.	COM.	MAX. KSI	MIN. KSI	RANGE KSI	V	TOT	EL	IN	PP	PC	CP	CC			
(A) Basic SRP Data																	
HRSC	0.50	0	0	179.3	-193.8	373.1	-0.039	2.388	1.492	0.896	0.896	0	0	0	43	0.02	
HRSC	0.50	0	0	140.6	-148.1	288.7	-0.025	1.523	1.155	0.368	0.368	0	0	0	200	0.11	
HRSC	0.50	0	0	109.6	-114.9	224.5	-0.023	1.052	0.898	0.154	0.154	0	0	0	756	0.42	
HRSC	0.50	0	0	111.2	-113.1	224.3	-0.008	1.002	0.898	0.104	0.104	0	0	0	1,322	0.71	
HRSC	0.50	0	0	99.8	-99.9	199.7	0	0.888	0.799	0.089	0.089	0	0	0	2,695	1.50	
HRSC	0.50	0	0	100.0	-100.0	200.0	0	0.837	0.800	0.037	0.037	0	0	0	4,205	2.24	
HRSC	0.50	0	0	97.8	-98.0	195.8	0	0.815	0.783	0.032	0.032	0	0	0	5,745	3.20	
HRSC	0.50	0	0	88.0	-87.7	175.7	0	0.721	0.703	0.018	0.018	0	0	0	25,433	13.60	
HRSC	0.50	0	0	81.8	-81.2	163.0	0	0.663	0.652	0.011	0.011	0	0	0	59,121	31.60	
CCCR	0.00065	0	1470	140.0	-101.3	241.3	+0.163	1.589	0.966	0.623	0.269	0.354	0	0	62	26.30	
CCCR	0.0031	0	285	136.0	-104.6	240.6	+0.131	1.265	0.962	0.303	0.151	0.152	0	0	226	20.20	
CCCR	0.0023	0	428	142.6	-90.8	233.4	+0.222	1.124	0.933	0.191	0.083	0.108	0	0	345	42.50	
CCCR	0.011	0	72	127.3	-90.4	217.7	+0.174	0.943	0.871	0.072	0.027	0.045	0	0	741	18.90	
CCCR	0.003	0	327	124.1	-50.4	174.5	+0.424	0.752	0.698	0.054	0.022	0.032	0	0	1,285	119.90	
CCCR	0.0096	0	76	111.4	-79.2	190.6	+0.169	0.807	0.762	0.045	0.016	0.029	0	0	1,400	40.50	
TCR	0.0017	572	0	101.7	-167.4	269.1	-0.244	1.444	1.076	0.368	0.160	0	0.208	0	103	16.90	
TCR	0.0066	130	0	84.4	-149.1	233.5	-0.277	1.091	0.934	0.157	0.082	0	0.075	0	458	19.20	
TCR	0.018	43	0	63.8	-125.5	189.3	-0.326	0.805	0.757	0.048	0.024	0	0.024	0	8,805	139.30	
BCCR	0.00034	744	2220	106.5	-106.5	213.0	0	1.492	0.851	0.641	0.160	0	0	0.481	114	93.80	
BCCR	0.0013	212	569	96.5	-97.8	194.3	-0.005	1.112	0.777	0.335	0.096	0	0	0.239	176	38.20	
BCCR	0.0099	42	59	87.7	-74.3	162.0	-0.081	0.718	0.648	0.070	0.026	0	0	0.044	3,550	107.00	
(B) Mean Stress Data																	
HRSC	0.50	0	0	130.6	-126.3	256.9	+0.017 ^(a)	1.188	1.028	0.160	0.160	0	0	0	435	0.24	
HRSC	0.50	0	0	109.4	-88.9	198.3	+0.103 ^(b)	0.835	0.793	0.042	0.042	0	0	0	1,626	0.90	
HRSC	0.50	0	0	78.5	-126.6	205.1	-0.235 ^(b)	0.859	0.820	0.039	0.039	0	0	0	4,812	2.58	
HRSC	0.50	0	0	118.5	-81.5	200.0	+0.185	0.804	0.800	0.004	0.004	0	0	0	2,813	1.50	
HRSC	0.50	0	0	108.7	-54.3	163.0	+0.333	0.652	0.652	<0.001	<0.001	0	0	0	22,775	12.70	
HRSC	0.50	0	0	140.0	-23.0	163.0	+0.718	0.652	0.652	<0.001	<0.001	0	0	0	12,168	6.50	
HRSC	0.50	0	0	163.0	+48.0	115.0	+1.833	0.460	0.460	<0.001	<0.001	0	0	0	633	0.35	
HRSC	0.50	0	0	140.0	0	140.0	+1.000	0.560	0.560	<0.001	<0.001	0	0	0	33,390	17.80	
HRSC	0.50	0	0	124.0	0	124.0	+1.000	0.496	0.496	<0.001	<0.001	0	0	0	68,143	36.40	
HRSC	0.50	0	0	115.0	0	115.0	+1.000	0.460	0.460	<0.001	<0.001	0	0	0	173,136	92.49	
HRSC	0.50	0	0	163.0	0	163.0	+1.000	0.652	0.652	<0.001	<0.001	0	0	0	1,615	0.90	
HRSC	0.50	0	0	81.5	-118.5	200.0	-0.184	>0.800	0.800	--	--	0	0	0	6,517	3.50	
HRSC	0.50	0	0	81.5	-101.5	183.0	-0.111	>0.732	0.732	--	--	0	0	0	20,639	11.00	
HRSC	0.50	0	0	70.0	-93.0	163.0	-0.142	0.652	0.652	<0.001	<0.001	0	0	0	68,818	36.70	

(a) $V_e = -1.0$ (b) $V_e = +1.0$

The PP life relation is shown in Fig. 4 as a straight line drawn through the PP inelastic strain range-cyclic life results. The same 0.5 Hz tests provided the necessary information to construct the stress range-cyclic life and the cyclic stress-strain relations shown in Figs. 5 and 6, respectively.

Establishment of the SRP inelastic strain range-cyclic life relations for CC, CP, and PC was accomplished by adhering strictly to the validity criteria and procedures prescribed in Ref. 3. These relations represent the behavior one would expect if it were possible to conduct tests with pure CC, CP, and PC inelastic strain ranges, i.e., no time-independent plastic strain present in either the tensile or compressive halves of the cycle for the CC-type tests, and none in the tensile half or none in the compressive half for the CP- and PC-types of cycles, respectively. The hysteresis loops one might expect from such idealized tests are those shown in Fig. 2. Since those conditions could only be approached in extremely long

time tests, it was considered desirable to conduct shorter time tests and use a damage rule to separate analytically the unwanted effects of the damage done by the PP strain range component.

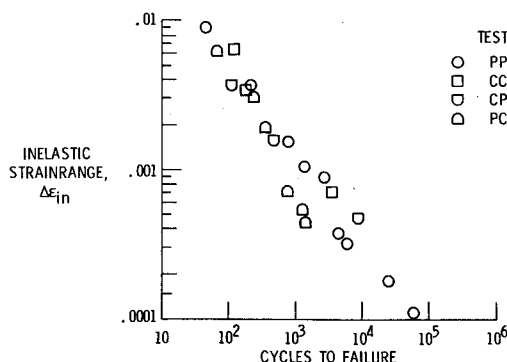
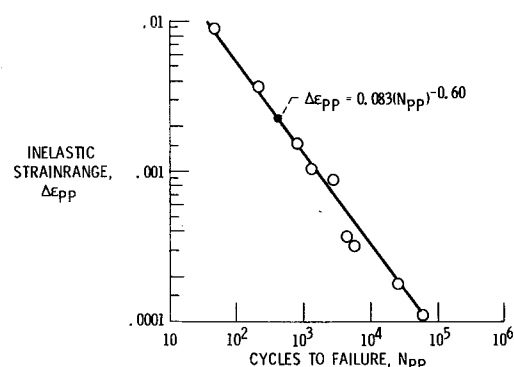
The four basic SRP life relations so established are displayed in Fig. 7 and can be expressed as:

$$\Delta\epsilon_{PP} = 0.083 (N_{PP})^{-0.60} \quad (1)$$

$$\Delta\epsilon_{CC} = 0.088 (N_{CC})^{-0.60} \quad (2)$$

$$\Delta\epsilon_{CP} = 0.056 (N_{CP})^{-0.60} \quad (3)$$

$$\Delta\epsilon_{PC} = 0.754 (N_{PC})^{-1.09} \quad (4)$$

Fig. 3 Inelastic strain range-life results for AF2-1DA at 1400°F, $V_e = 0$.Fig. 4 PP life relation for AF2-1DA at 1400°F, 0.5 Hz, $V_e = 0$.

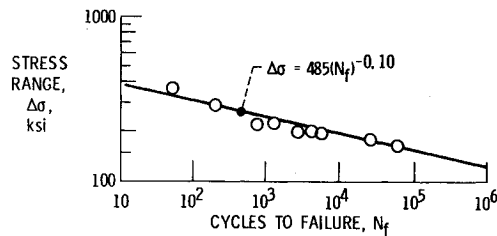


Fig. 5 Stress range-life relation for AF2-1DA at 1400°F, 0.5 Hz, $V_\epsilon = 0$.

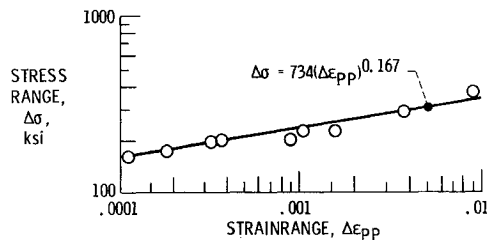


Fig. 6 Cyclic stress-strain curve for AF2-1DA at 1400°F, 0.5 Hz, $V_\epsilon = 0$.

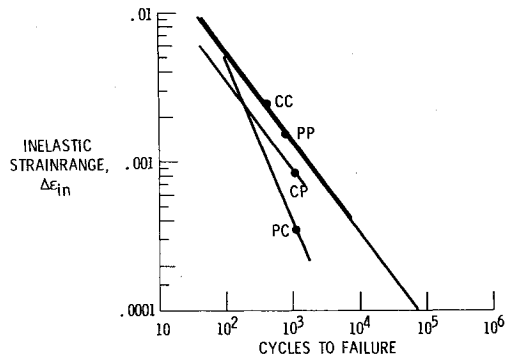


Fig. 7 SRP life relations obtained without consideration of mean stress effects, AF2-1DA at 1400°F and $V_\epsilon = 0$.

The slope of the PC life relation is much steeper than that for the other relations, and is steeper than any the authors have observed for any alloy. The coefficient of 0.754 is nearly an order of magnitude larger than the other coefficients and is even three times as great as the tensile ductility (see Table 1). The PC test points responsible for the extreme steepness of the slope and the resultant increase in the coefficient are the ones at inelastic strain range levels of less than 0.001, and for which tensile mean stresses are present.

Therefore, the question arises as to whether or not these mean stresses are responsible for the low observed lives and the steep slope of this line. There is also the much broader question as to the influence of mean stress in the presence of cyclic inelastic strain, especially when the mean stresses are a natural result of the inelastic constitutive behavior of the material. In fact, if there were no inelastic strains present in these tests, there would be no mean stresses generated, since the total strain ranges are completely reversed about a zero mean strain. In an attempt to answer the questions posed above, a supplementary mean stress testing program was initiated, the planning and results of which are described in the following section.

Mean Stress Considerations

Elastic Behavior

Consideration of the presence of and the effect on cyclic life of mean stresses is usually associated with nominally elastic loading conditions such as found in the high-cycle fatigue

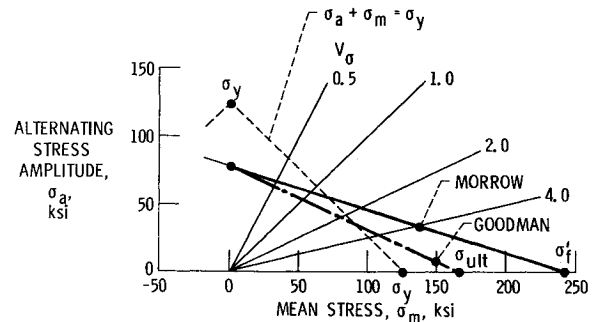
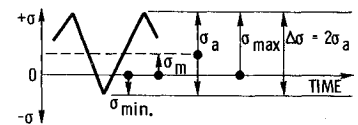


Fig. 8 Theoretical alternating-mean stress diagrams for AF2-1DA at 1400°F; curves shown for 10^5 cycles to failure.

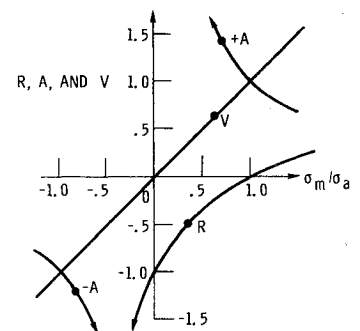


$$R = \frac{\sigma_{\min}}{\sigma_{\max}} = \frac{1 - A}{1 + A} = \frac{V - 1}{V + 1}$$

$$A = \frac{\sigma_a}{\sigma_m} = \frac{1 - R}{1 + R} = \frac{1}{V}$$

$$V = \frac{\sigma_m}{\sigma_a} = \frac{1 + R}{1 - R} = \frac{1}{A}$$

Fig. 9 Relations between mean stress parameters.



regime. The effect of mean stress on endurance limits has been a matter of practical concern for nearly a century, and numerous mean stress-alternating stress equations have been proposed. Names such as Goodman, Gerber, and Soderberg are prevalent in the high-cycle fatigue literature of the past. More recently, Morrow¹⁰ proposed an approach that retained the simplicity of the Goodman diagram, while more accurately representing the available data. In the present paper, the Morrow concept has been adopted as a basis for studying mean stress effects, but writing the basic mean stress-alternating stress-fatigue life equation in terms of cycles to failure N_f , rather than reversals to failure $2N_f$. Hence, the mean stress fatigue equation is written as:

$$\Delta\sigma = 2(\sigma_f' - \sigma_m)N_f^{-b} \quad (5a)$$

From Fig. 5, the value of b is 0.10 and $\sigma_f' = 243$ ksi for $\sigma_m = 0$. Expressing Eq. (5a) in terms of the stress amplitude σ_a , we have

$$\sigma_a = (243 - \sigma_m)N_f^{-0.10} \quad (5b)$$

This equation is labeled as the Morrow equation in Fig. 8, where a comparison can be drawn with the Goodman line for a cyclic life of 10^5 . For reference purposes, the locus of the static 0.2% offset yield strength is also shown.

Lines radiating from the origin of the figure represent constant ratios of the mean-to-alternating stress V_σ . The quantity V is simply the inverse of the familiar A ratio commonly used to describe states of mean stress. Use of the term V in this paper is preferable to either of the more commonly used A or R ratios, since V is more directly associated with the mean stress. It carries the same sign as the mean stress, is zero when the mean stress is zero, and as the mean stress increases, V increases in direct proportion. The definitions of and interrelationships between V , A , and R are shown in Fig. 9.

A useful expression can be derived from Eq. (5a) which can be used in dealing with mean stress effects. Consider two elastic loading conditions for which the alternating stress amplitudes (or stress ranges) are identical. In one, let the mean stress be zero and the corresponding life be labeled N_{f0} .

In the other, a tensile or compressive mean stress is assumed present and the corresponding life is designated N_{fm} .

Then

$$\sigma_a = (\sigma_f' - \sigma_m) N_{fm}^{-b} \quad (5c)$$

and

$$\sigma_a = \sigma_f' N_{f0}^{-b} \quad (5d)$$

Solving for σ_f' from Eq. (5d), substituting into (5c), and further recognizing that $\sigma_m = V_\sigma \sigma_a$,

$$\sigma_a = (\sigma_a N_{f0}^b - V_\sigma \sigma_a) N_{fm}^{-b} \quad (6)$$

By cancelling σ_a and rearranging terms, we arrive at

$$N_{fm}^b = N_{f0}^b - V_\sigma \quad (7)$$

Equation (7) expresses the conclusion that the only material property needed to relate cyclic life with and without a mean stress is the slope of the stress amplitude (or range) vs life curve. In Morrow's terminology, this material property is called the "fatigue strength exponent."

The potential use for Eq. (7) may be greater than implied by the assumptions. For example, if the presence of a mean stress does not alter the cyclic stress-strain relation, then the assumption of equal stress amplitudes would also imply equal strain ranges. Thus, Eq. (7) could possibly be used for inelastic strain cycling conditions. This aspect will be explored in a subsequent section.

The load-controlled (HRLC) mean stress fatigue life data listed in Table 2(b) were generated for the purpose of evaluating the validity of Eq. (7). Rather than trying to predict the lives of the tests with different mean stresses, the reverse approach was taken in which the observed lives with mean stresses N_{fm} were used, along with the mean stress ratio to calculate the life that would have existed without the mean stresses present. In this way, all of the mean stress results could be superimposed on the zero mean stress fatigue curve taken from Fig. 5. The results are shown in Fig. 10 where it is seen that Eq. (7) has been able to successfully collapse the mean stress results onto the original zero mean stress fatigue curve. Having thus verified the validity of Eq. (7) for the nominally elastic loading conditions considered, its applicability to cycling conditions involving more significant amounts of inelastic strain per cycle can be investigated.

Inelastic Behavior

Mean stresses may exert significant influences on cyclic life in the high-cycle, nominally elastic fatigue regime, but it would seem highly unlikely that similar effects could be

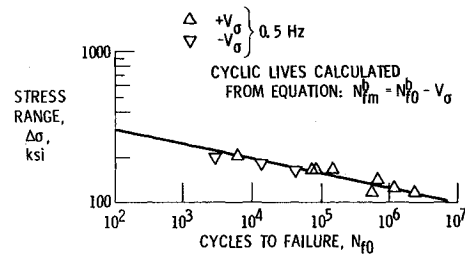


Fig. 10 Mean stress fatigue results corrected to a zero mean stress condition, AF2-1DA at 1400°F.

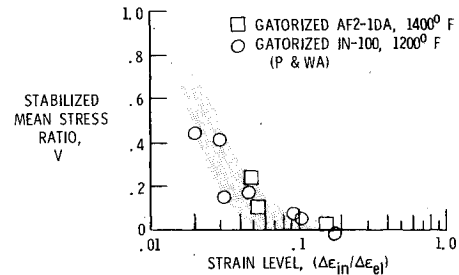


Fig. 11 Effect of strain level on ability of materials to retain or wash-out mean stresses during nonreversed continuous strain cycling.

carried over into the low-cycle, highly inelastic fatigue regime. It is not even possible here to sustain mean stresses, except under very specialized conditions such as, for example, those encountered in the CP- and PC-types of SRP test cycles shown in Fig. 2. Thus, it was assumed that there exists some straining level below which mean stresses will exert their full influence, as indicated by Eq. (7), but above which their influence is washed out by the presence of cyclic inelastic deformation. A logical choice for this level of straining is the point for which the inelastic strains are large enough that mean stresses cannot be sustained during continuous strain cycling. As a measure of the straining level, the ratio of the inelastic to the elastic strain ranges was selected, although it is recognized that other possible choices exist. An examination of the results in Table 2(b) for the three HRSC tests (which were conducted with mean strain ratios V_ϵ of either +1.0 or -1.0) shows that if the straining level ($\Delta\epsilon_{in}/\Delta\epsilon_{el}$) is above approximately 0.1, the mean stress is washed out. If it is below, some of the initially induced mean stress is retained. A comparison of the observed lives of these tests with the PP life relation previously established in Fig. 4 does indeed show an effect on life due to the retained mean stress, even though some inelastic strain is present. Further documentation of the above observations can be found in the 1200°F results obtained with Gatorized IN-100 reported by VanWanderham et al.¹¹ They conducted continuous strain cycling fatigue tests with $V_\epsilon = +1.0$ and found that the initially induced mean stresses would wash out to essentially zero if the straining level was large enough, but at lower strains, a significant portion of the tensile mean stress could be retained. Figure 11 displays the results for both Gatorized alloys. A strain level of $\Delta\epsilon_{in}/\Delta\epsilon_{el} = 0.10$ represents the demarcation point above which mean stresses need not be considered, and below which they must.

Rather than apply an abrupt step-function to the stress ratio V_σ in Eq. (7) as the strain level passes through the 0.1 demarcation point, it was deemed advisable to provide for a smooth, but nevertheless rapid, transition using a function called k . The selection of this function is somewhat arbitrary—the important aspect being to provide a smooth transition that goes between zero and unity within a relatively narrow range of the demarcation point. The selected function is shown in Fig. 12. Returning to Eq. (7) and substituting V_{eff}

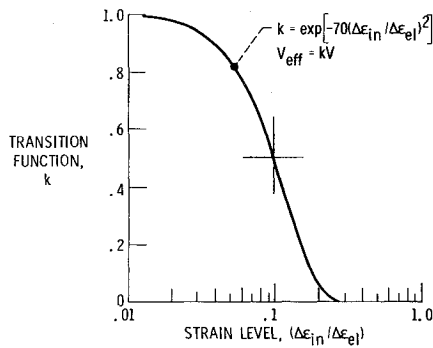


Fig. 12 Transition function used to relate the effective and actual mean stress ratios.

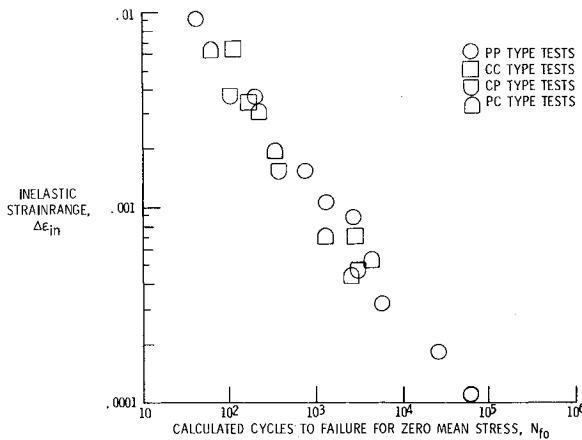


Fig. 13 Inelastic strain-range-life results for AF2-1DA at 1400°F, $V_{\epsilon} = 0$; cycles to failure corrected to a zero mean stress condition.

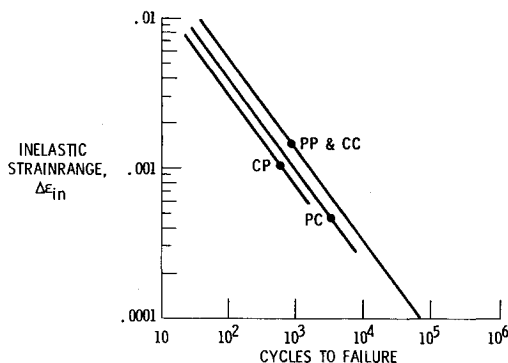


Fig. 14 SRP life relations corrected to a zero mean stress condition, AF2-1DA at 1400°F.

for V_{σ} , where $V_{\text{eff}} = kV_{\sigma}$,

$$N_{fm}^b = N_{f0}^b - V_{\text{eff}} \quad (8)$$

Equation (8) is thus assumed to reflect the mitigating influence of cyclic inelastic strains on the effectiveness of mean stresses, at least for continuous strain cycling conditions.

Zero Mean Stress SRP Results

Equation (8) was applied directly to the basic SRP data presented at the beginning of this paper in an attempt to derive a set of SRP life relations that represent a hypothetical zero mean stress condition. The first step was to use Eq. (8) to calculate the value of N_{f0} for each of the basic SRP tests listed in Table 2 using the tabulated values of V , $\Delta\epsilon_{in}$, $\Delta\epsilon_{el}$, and N_f (in this case, equal to N_{fm}).

Figure 13 depicts the results of the N_{f0} calculations as applied to the data of Fig. 3. It is observed here that the mean stress correction has consolidated the creep-fatigue results into a narrower band than found in Fig. 3. Furthermore, the relative positions of the data points are more in keeping with previous experience of the authors.

Once N_{f0} was known, it was treated as if it were an experimentally determined life. From that point on, the procedures for establishing the CC, CP, and PC inelastic SRP life relationships were exactly the same as used earlier in this paper. The results of these calculations are the set of SRP life relations shown in Fig. 14 that represent a condition of zero mean stress.

The equations of the straight lines are:

$$\Delta\epsilon_{PP} = 0.083 (N_{PP})^{-0.60} \quad (\text{unchanged}) \quad (9)$$

$$\Delta\epsilon_{CC} = 0.083 (N_{CC})^{-0.60} \quad (10)$$

$$\Delta\epsilon_{PC} = 0.063 (N_{PC})^{-0.60} \quad (11)$$

$$\Delta\epsilon_{CP} = 0.049 (N_{CP})^{-0.60} \quad (12)$$

The slopes and coefficients of the above equations agree more closely with the authors' previous experience with other alloys than do the slopes and coefficients for the life relationships presented earlier in the paper and for which mean stresses were totally ignored. The authors' previous experience is reflected by the Ductility Normalized=(DN) SRP life relations.¹² These relationships were determined from a correlation among a large body of measured SRP data (for which, as discussed earlier, mean stress effects were essentially absent) and tensile plastic ductility (D_p) and creep-rupture ductility (D_c) for the specific materials involved. The reader should consult Ref. 12 for further details of the DN-SRP equations.

The slope used in all of the DN-SRP equations is -0.60 , just as found in the present study. The coefficients in the DN-SRP equations are a function of D_p for the PP and PC life relations, whereas a function of D_c is used for the CC and CP life relations. D_p and D_c can be computed from the percent reduction of area values listed in Table 1— $D_p = 0.252$ and $D_c = 0.163$.

Thus, the DN-SRP equations evaluated for Gatorized AF2-1DA at 1400°F are:

$$\Delta\epsilon_{PP} = 0.126 (N_{PP})^{-0.60} \quad (13)$$

$$\Delta\epsilon_{CC} = 0.084 (N_{CC})^{-0.60} \quad (14)$$

$$\Delta\epsilon_{PC} = 0.063 (N_{PC})^{-0.60} \quad (15)$$

$$\Delta\epsilon_{CP} = 0.069 (N_{CP})^{-0.60} \quad (\text{transgranular cracks}) \quad (16a)$$

or

$$\Delta\epsilon_{CP} = 0.034 (N_{CP})^{-0.60} \quad (\text{intergranular cracks}) \quad (16b)$$

A comparison of the DN-SRP equations with the zero mean stress SRP equations shows some remarkable similarities. In fact, the PC life relation, which involved the greatest mean stress correction, is identical for the two cases. Although this is only circumstantial evidence, it does support the notion that the mean stresses have been appropriately accounted for by Eq. (8).

An important item when applying the zero mean stress SRP life relations to the life prediction of a general inelastic strain cycle is the order of accounting for creep-fatigue effects and mean stress effects. The order is crucial, and requires as the first step that the conventional SRP analysis be performed

and a cyclic life thereby predicted. This life represents the N_{fo} life. If the cycle under analysis has a mean stress present, its effect is determined from the value of k and the resultant V_{eff} is used to determine the life N_{fm} , which represents the predicted life for the cycle in question. Note that the reverse order of calculations was used when raw data were analyzed for the purpose of establishing a zero mean stress SRP life relation.

At least one other investigator has indirectly considered the effects of mean stress in the creep-fatigue regime. In Ostergren's approach,¹³ the peak tensile stress appears in a revised form of Coffin's frequency modified equation.⁶ However, there is no one-to-one correspondence between mean stress and peak tensile stress in the creep-fatigue regime, so it is difficult to compare the current approach with that of Ostergren. The data presented in Table 2 are, however, amenable to analysis by the Ostergren approach.

A paper dealing with a novel approach to the problem of mean stress effects in gas turbine disks has been presented recently by Cruse and Meyer.¹⁴ However, this paper does not delve into the high-temperature creep-fatigue aspects of the problem, nor is consideration given to the application of the approach to conditions involving measurable cyclic inelastic deformations.

Summary and Concluding Remarks

In the process of evaluating the high-temperature, low-cycle, creep-fatigue behavior of the alloy AF2-1DA, mean stress effects were encountered, which under certain conditions were of greater importance in governing cyclic life than the simultaneously imposed creep effects. The method of SRP was used to represent the creep-fatigue effects.

A procedure was proposed for dealing with the mean stress effects prior to the determination of the SRP characteristics. Such a procedure resulted in a set of SRP life relations representative of a zero mean stress condition. In applying these relations to the life prediction of a general creep-fatigue cycle, the conventional SRP life analysis procedures can thus be followed and the life calculated. That life is then adjusted through the use of Eq. (8) to reflect the effect of the mean stress present in the cycle of interest.

The analysis for dealing with mean stresses proposed in this paper is based upon limited data, and as more information becomes available, refinements or simplifications may well result. For example, the particular form selected for the transition function k , and the location of the strain level demarcation point (above which mean stress effects are unimportant) may be different for other materials or conditions. The basic concept, however, appears to be sound.

It is recognized that there is still a need to consider other aspects of mean stress effects in high-temperature, creep-fatigue problems. This is especially true for thermal fatigue

cycling during which both the temperature-dependent modulus and yield strength will invariably produce mean stresses. The effect of these mean stresses is questionable, not only in the inelastic cycling regime, but also in the totally elastic regime. It would seem at this time that mean effects in thermal fatigue could better be described in terms of the *mean elastic strains* than in terms of the mean stresses. These two terms differ because the modulus of elasticity is a function of temperature. For the isothermal conditions considered in the present investigation, however, the two terms are identical.

References

- ¹Manson, S.S., Halford, G.R., and Hirschberg, M.H., "Creep-Fatigue Analysis by Strainrange Partitioning," *Symposium on Design for Elevated Temperature Environment*, ASME, 1971, pp. 12-28.
- ²Manson, S.S., "The Challenge to Unify Treatment of High Temperature Fatigue—A Partisan Proposal Based on Strainrange Partitioning," STP-520 ASTM, 1973, pp. 744-782.
- ³Hirschberg, M.H. and Halford, G.R., "Use of Strainrange Partitioning to Predict High-Temperature Low-Cycle Fatigue Life," NASA TN D-8072, 1976.
- ⁴Hirschberg, M.H., "A Low-Cycle Fatigue Testing Facility," STP-465, ASTM, 1969, pp. 67-86.
- ⁵Boiler and Pressure Vessel Piping Code Case 1592, Sec. III, ASME, 1974.
- ⁶Coffin, L.F. Jr., "Fatigue at High Temperature," STP-520, ASTM, 1973, pp. 5-34.
- ⁷Majumdar, S. and Maiya, P.S., "A Damage Equation for Creep-Fatigue Interaction," *ASME-MPC Symposium on Creep-Fatigue Interaction*, 1976, pp. 323-335.
- ⁸Drapier, J.M., Final Discussion Summary, *Characterization of Low Cycle High Temperature Fatigue by the Strainrange Partitioning Method*, AGARD Conf. Proc. No. 243, 1978, pp. D4-1-11.
- ⁹Saltsman, J.F. and Halford, G.R., "Application of Strainrange Partitioning to the Prediction of Creep-Fatigue Lives of AISI Types 304 and 316 Stainless Steel," *Transactions of the ASME, Series J*, Vol. 99, No. 2, May 1977, pp. 264-271.
- ¹⁰Morrow, J., "Fatigue Properties of Metals," *Fatigue Design Handbook*, Sec. 3.2, SAE Advances in Engineering, Vol. 4, 1968, pp. 21-29.
- ¹¹VanWanderham, M.C., Wallace, R.M., and Annis, C.G., "Low Cycle Fatigue of IN-100: Strainrange Partitioning Method," *AGARD Conference Proceedings*, No. 243, 1978, pp. 3-1-17.
- ¹²Halford, G.R., Saltsman, J.F., and Hirschberg, M.H., "Ductility Normalized-Strainrange Partitioning Life Relations for Creep-Fatigue Life Prediction," *Proceedings of the Conference on Environmental Degradation of Engineering Materials*, V.P.I. & State Univ., Blacksburg, Va., 1977, pp. 599-612.
- ¹³Ostergren, W.J., "Correlation of Hold Time Effects in Elevated Temperature Low-Cycle Fatigue using a Frequency Modified Damage Function," *ASME-MPC Symposium on Creep-Fatigue Interaction*, Dec. 1976, pp. 179-202.
- ¹⁴Cruse, T.A. and Meyer, T.G., "A Cumulative Fatigue Damage Model for Gas Turbine Engine Disks Subjected to Complex Mission Loading," ASME 78-WA/GT-14A, presented at ASME Winter Annual Meeting, San Francisco, Calif., Dec. 1978.